Quantum Information Review
An International Journal

http://dx.doi.org/10.12785/qir/010201

Non-Markovian Dynamics of Entanglement of three-level atom embedded in a 3D photonic band gap structure

M. S. Ateto[1,2,*]

[1] Mathematics Department, Faculty of Science at Qena, South Valley University, 83523 Qena, Egypt
[2] Mathematics Department, Faculty of Science, Gazan University, Gazan, Kingdom of Saudi Arabia

Received: 7 Feb. 2013, Revised: 9 Jun. 2013, Accepted: 13 Jun. 2013
Published online: 1 Jul. 2013

Abstract: Entanglement evolution for a classically pumped three-level atom interacting with an anisotropic structured reservoir is studied. We demonstrate that entanglement decay is much slower in the reservoir with the memory effects. This point is beneficial for the implementation of quantum computation in the non-Markovian environments. Unlike the free-space case, the unusual reservoir stimulates stationary entanglement with amplitude depends strongly on the relative phase between the control laser coupling the two upper levels and the pump laser pulse used to create an excited state of the atom in a coherent superposition of the two upper levels. An optimal stationary degree of entanglement is achieved for negative relative phase, where both detunings - from the upper band gap and driving laser - are the same. Moreover, a significant stationary degree of entanglement is reached, for high detuned upper levels with the pump laser pulse, on resonant frequency near the edge of the PBG. For entanglement in stationary regime, the Rabi frequency of the control laser field exceeds the rate of entanglement degradation or enhancement for tuned or detuned frequency from the band gap, depending on the relative phase value.

Keywords: Non-Markovian; anisotropy; Photonic structure; Dispersion; Entanglement; Steady state.

1 Overview

Entanglement [1,2,3,4,5,6], a characteristic feature of quantum mechanics, plays a key role in many quantum information tasks [7]. In order to implement those tasks, one hopes that entanglement needed to be maintained for sufficiently long time to fulfill the design. However, entanglement is easily degraded due to the unwanted interaction between the system and its environment, where, decoherence of quantum entanglement is usually inevitable [8]. Therefore, creating a long-lived entanglement and avoiding disentanglement in a practical way are what count in realistic quantum information protocols. It would seem important to stabilize quantum systems against this unwanted phenomenon. To achieve this goal, it is efficient to devise schemes for the creation of entangled states and to observe their dynamical characteristics in the presence of environmental effects. For a long time, the essential target of many proposals was the control and manipulation of the quantum information stored in the system while keeping the detrimental environmental effects low [9,10,11,12,13]. Therefore, dynamical properties of quantum entanglement have received much attention [14,15,16,17, 18,19,20]. It is well-known that the radiation properties of atoms can dramatically be manipulated by changing the environment where atoms emit photons. It is therefore desirable to investigate the entanglement of the three-level systems under environmental effects. The decay of a three-level atom system with one shared excitation is a fundamental problem of some importance. In most cases, analytic progress can only be made under the Markovian hypothesis, which requires decay of correlation between the system and the environment [21, 22]. In addition, the Markovian approximation is used for the study of dynamics of quantum systems that weakly coupled to reservoirs without memory effects [23]. However, in realistic environments with memory effects, time evolutions of quantum systems often obey the non-Markovian dynamics. In this important case, possibility of periodic re-excitation of the atom by the spontaneously radiated field is allowed, hence, the reservoir can be treated in a non-Markovian fashion in the sense that energy is radiated into the field by the atom and

* Corresponding author e-mail: mohammed.ateto@gmail.com; mohamed.ali11@sci.svu.edu.eg

can be at least partially recovered by the atom again [9]. In addition, in non-Markovian case, the information transferred to the reservoirs is fed back to the atoms due to the memory effect, which means the excited atomic state will arise again [24]. For periodic dielectric media predicted [25,26] that a suppression of spontaneous emission can be achieved. This means that, the entanglement-induced memory effects can persist for arbitrary long times and affect the relaxation to equilibrium, hence, strong non-exponential behavior can arise.

Our aim, in this article, is to identify those circumstances that allow for generating long-lived entanglement, while filtering out decoherence effects, and are therefore highly advantageous for optical communications, data storage and processing, near or at the quantum limit. Our scheme depends on the coherent control by an external driving field and photon localization by an action on spontaneous emission from a three-level atom by locating the atom into a photonic band structure (PBS). The atom and its unusual (structured) reservoir now evolve as an effective two-qubit system. With the full development and application of cooling and trapping techniques on atoms, controlling entanglement by applying laser field has become the popular subject [27]. Note, the purely classical field is not able to generate any kind of quantum correlation between two subsystems [28].

PBS, also referred to as photonic crystals (PCs), provide an important tool to realize, a strong localization at the classical level and trapping, of light in bulk material [29], and the complete inhibition of spontaneous emission [30] over a broad frequency range. Moreover, the driving of a multi-level atom with a sufficiently strong resonant field alters the radiative dynamics in a fundamental way, even in ordinary vacuum. In view point of quantum information, the protected electric dipole within the PBS provides a basis for a qubit to encode information for quantum computations. It is demonstrated that [21], storage of quantum information in a single three-level atom is facilitated by the localization of light in the vicinity of the atom, suggesting an application of the model system as a memory device on the atomic scale. For further detailed literature on the nature, fabrication and applications of PBS see Refs. [29,30,21] and papers therin. For such reasons, three-level atoms are of particular interest in quantum optics and predictably their behavior in the context of structured reservoirs has been addressed [31,32].
The paper is organized as follows: Section 2 contains a description of the system Hamiltonian and the derived the equations of motion for the amplitudes involved in the wavefunction of the system atom+continuum. In section 3, we derived the reduced density operator used to calculate entanglement measure we are going to use and give a brief survey about this measure. In section 4 the dynamical behavior of the system in free space, supported with a sample case, is thus investigated followed by analysis of the obtained results. In section 5 the same problem is placed in the context of a photonic band structure, while two special cases are considered, i.e, PBS model with anisotropic dispersion relation and stationary regime of evolution. The results are summarized in section 6.

2 Model Hamiltonian in the interaction picture and equations of motion

The interaction of a multi-mode quantized field of frequency ω_k with a single pumped three-level atom is described by the Hamiltonian

$$\widehat{\mathrm{H}} = \sum_{i=0}^{2} \hbar\omega_i\sigma_{ii} + \sum_{k,\lambda} \hbar\omega_k a^{\dagger}_{k\lambda} a_{k\lambda}$$
$$+ i\hbar\Omega\left(\sigma_{12}e^{i(\omega_L t+\phi_L)} - \sigma_{21}e^{-i(\omega_L t+\phi_L)}\right)$$
$$+ i\hbar\sum_{k,\lambda} g_{k\lambda}\left(\widehat{a}^{\dagger}_{k\lambda}\sigma_{02} - \sigma_{20}\widehat{a}_{k\lambda}\right), \quad (1)$$

We let $|0\rangle$, $|1\rangle$ and $|2\rangle$ denote, respectively, the ground, and the two excited levels of the atom. The quantities ω_L, Ω and ϕ_L define, respectively, the angular frequency, the Rabi frequency and the phase of the driving laser.
The first two terms of Eq.(1), whose sum denotes the Hamiltonian of the unperturbated system, $\widehat{\mathrm{H}}_0$, stand, repectively, for the Hamiltonians of the bare atom and the photon reservoir (neglecting the zero-point energy) with a large amount of independent harmonic oscillators. The last two terms, whose sum denots the Hamiltonian of the perturbated system , $\widehat{\mathrm{H}}_1$, respectively represent the Hamiltonian, $\widehat{\mathrm{H}}_{AL}$, of the interaction between the atom and the coherent monochromatic laser field driving the transition $|2\rangle \rightarrow |1\rangle$, and that, $\widehat{\mathrm{H}}_{AR}$, of the interaction between the atomic transition $|2\rangle \rightarrow |0\rangle$ and the environment, with $\widehat{a}^{\dagger}_{k\lambda}$ and $\widehat{a}_{k\lambda}$ are the creation and annihilation operators of the reservoir, via the electronic transition dipole moment $\hat{\mathbf{d}}_{20}$ with the frequency-dependent coupling constant (assumed to be real), $g_{k\lambda} = \omega_{20} d_{20}\, \hat{\mathbf{e}}_{k\lambda}.\hat{\mathbf{d}}_{20}/\sqrt{2\omega_k\varepsilon_0 V}$.

Working in the interaction picture, the interaction version $\widehat{\mathrm{H}}_{\mathrm{int}} = e^{i\widehat{\mathrm{H}}_0 t/\hbar}\widehat{\mathrm{H}}_1 e^{-i\widehat{\mathrm{H}}_0 t/\hbar}$, of the system Hamiltonian (1) reads

$$\widehat{\mathrm{H}}_{\mathrm{int}} = i\hbar\Omega\left(\sigma_{12}e^{i(\mu_L t+\phi_L)} - \sigma_{21}e^{-i(\mu_L t+\phi_L)}\right)$$
$$+ i\hbar\sum_{k,\lambda} g_{k\lambda}\left(\widehat{a}^{\dagger}_{k\lambda}\sigma_{02}e^{i\mu_k t} - \sigma_{20}\widehat{a}_{k\lambda}e^{-i\mu_k t}\right), \quad (2)$$

where $\mu_L = \omega_L - \omega_{21}$ is the relative detuning of the upper transition $|2\rangle \rightarrow |1\rangle$ from driving laser and $\mu_k = \omega_k - \omega_{20}$ is the detuning of the radiation mode frequency ω_k from the atomic transition frequency ω_{20}. We proceed to solve the Schrödinger equation of motion for $|\psi(t)\rangle$, i.e.,

$$|\dot{\psi}(t)\rangle = -i\,\widehat{\mathrm{H}}_{\mathrm{int}}\,|\psi(t)\rangle, \tag{3}$$

where $|\psi(t)\rangle$ is the state vector of the system any later time t, and can be written as

$$|\psi(t)\rangle = C_1(t)|1,\{0\}\rangle + C_2(t)|2,\{0\}\rangle$$

$$+\sum_{k,\lambda} B_{k\lambda}(t)|0,\{1_{k,\lambda}\}\rangle \tag{4}$$

Note, when there is no driving field, our model system can be viewed as a two-level system consisting of levels $|2\rangle$ and $|0\rangle$, with the transition frequency ω_{20}.
The equations of motion for the probability amplitudes $C_1(t)$, $C_2(t)$ and $B_{k\lambda}(t)$ are obtained by applying the Schrödinger equation (3), assuming $\hbar = 1$, as

$$\dot{C}_1(t) = \Omega C_2(t)e^{i(\mu_L t+\phi_L)}, \tag{5}$$

$$\dot{C}_2(t) = -\Omega C_1(t)e^{-i(\mu_L t+\phi_L)}$$

$$-\sum_{k,\lambda} g_{k\lambda}B_{k\lambda}(t)e^{-i\mu_k t}, \tag{6}$$

$$\dot{B}_{k\lambda}(t) = g_{k\lambda}C_2(t)e^{i\mu_k t}. \tag{7}$$

With the initial conditions, $B_{k\lambda}(0) = 0$ and $C_1(t=0) = C_1(0)$, it is not difficult to obtain

$$\dot{C}_2(t) = -\Omega C_1(t)e^{-i(\mu_L t+\phi_L)} - \int_0^t dt' C_2(t')F(t-t'), \tag{8}$$

where $F(t-t')$ is the memory kernel and given by

$$F(t-t') = \sum_{k,\lambda} g_{k\lambda}^2 e^{-i\mu_k(t-t')}, \tag{9}$$

The determination of the memory kernel is related to the reservoir spectral density [34].

3 The reduced density operator and entanglement measure

A major thrust of current research is to find an efficient and quantitative measure of entanglement for bipartite system. The concurrence [33,34], negativity, [35] and relative entropy [36] are some of these measures. Also, one of these approaches that based on the eigenvalue spectra of the system density matrices is entropy method [37,38,39]. Entropy, known as von Neumann entropy [37], is related to the density matrix, which provides a complete statistical description of the system. It is a commonly accepted fact that von Neumann entropy [37] is the unique entanglement measure for bipartite systems in a pure state [40]. In order to calculate the entropy $S(t)$, we must obtain the eigenvalues of the reduced density operator. Recalling Eq. (4), the full density matrix $\rho(t) = |\psi(t)\rangle\langle\psi(t)|$, needed for calculating the reduced density matrix $\rho_{\mathbf{A}}(t)$, after the tracing of the reservoir variables, is expressed as

$$\rho_{\mathbf{A}}(t) = \begin{pmatrix} \rho_{11} & \rho_{12} & 0 \\ \rho_{21} & \rho_{22} & 0 \\ 0 & 0 & \rho_{00} \end{pmatrix}, \tag{10}$$

where

$$\rho_{11} = |C_1(t)|^2, \quad \rho_{12} = C_1(t)C_2^*(t) = \rho_{21}^*,$$

$$\rho_{22} = |C_2(t)|^2, \quad \rho_{00} = \sum_{k,\lambda}|B_{k\lambda}(t)|^2. \tag{11}$$

In terms of the eigenvalues, χ_y, $(y = 1,2,3)$, entropy can be defined as follows [38,41]

$$S(\rho_{\mathbf{A}}) = -\sum_{y=1}^{3} \chi_y \ln \chi_y \tag{12}$$

where χ_y, $(y = 1,2,3)$ are the roots of the charactersic equation of degree three

$$\chi^3 - [\rho_{11}+\rho_{22}+\rho_{00}]\chi^2 + [\rho_{11}\rho_{22}+\rho_{00}(\rho_{11}+\rho_{22}) - |\rho_{12}|^2]$$

$$\chi + (|\rho_{12}|^2\rho_{00} - \rho_{11}\rho_{22}\rho_{00}) = 0 \tag{13}$$

The reduced density matrix is, however, calculated in a general form, hence, entropy of the system can be easily copmuted. The results will depend crucially on the shape of the memory kernel (9). To gain clearer insight, a comparison between various shapes of the memory kernel (9) is, however, efficient. This is precisely what is done in the next sections.

4 Entanglement in the Markovian regime

Markovian interactions, i.e., interactions with free space, are characterized by delta-function-dependent memory kernel [23]. Thus, for the electromagnetic vacuum which is characterized by the dispersion relation $\omega(k) = ck$, the memory kernel Eq. (9) takes the form

$$F(t-t') = \gamma_{20}\delta(t-t'), \tag{14}$$

where, $\gamma_{20} = \omega_{20}^3 d_{20}^2/(6\pi c^3 \varepsilon_0)$, is half the spontaneous emission rate Γ for the transition $|2\rangle \rightarrow |0\rangle$ in the Markovian model.

If initially the atom is in the coherent superposition of its two upper levels $|2\rangle$ and $|1\rangle$ where the radiation-field reservoir is initially in the vacuum state, the initial state atom-reservoir system can be expressed as

$$|\psi(0)\rangle = C_1(0)|1,\{0\}\rangle + C_2(0)|2,\{0\}\rangle, \qquad (15)$$

where, $C_1(0) = e^{i\phi_p}\sin(\theta)$ and $C_2(0) = \cos(\theta)$, with the parameter θ measures the degree of excitation of the levels $|2\rangle$ and $|1\rangle$. In this case, on using the initial condition (15) with Eqs. (5) and (8), the amplitudes $C_2(t)$ and $C_1(t)$ can be easily expressed, respectively, as

$$C_2(t) = \sum_{l=1}^{2} \frac{C_2(0)(s_l + i\mu_L) - \Omega C_1(0) e^{-i\phi_L}}{s_l - s_k}\, e^{x_l t}, \quad k = 1,2;\ l \neq k. \qquad (16)$$

$$C_1(t) = \sum_{l=1}^{2} \frac{\Omega e^{i\phi_L} C_2(0) - C_1(0)(s_k + i\mu_L)}{s_l - s_k}\, e^{(x_l + i\mu_L)t}, \quad k = 1,2;\ l \neq k. \qquad (17)$$

with

$$x_l = -\frac{\gamma_{20} + i\mu_L}{2} + (-1)^{l+1}\sqrt{\left(\frac{\gamma_{20} - i\mu_L}{2}\right)^2 - \Omega^2}, \quad l = 1,2. \qquad (18)$$

For resonance driving laser, $\mu_L = 0$, we can distinguish three stages in the dynamics of the populations and entropy according to the roots x_l. From equation (18), we have

$$x_l = \begin{cases} 1.\ \text{negative} & 2\Omega/\gamma_{20} \leq 1 \\ 2.\ \text{complex (with a real part equal to } -\gamma_{20}/2) & 2\Omega/\gamma_{20} > 1 \end{cases} \qquad (19)$$

In particular, when $2\Omega/\gamma_{20} = 1$, equation (18) has a double root $x_1 = x_2 = -\gamma_{20}/2$, and Eqs. (16, 17) reduced, respectively, to

$$C_2(t) = e^{-\frac{\gamma_{20}}{2}t}\left[C_2(0) - \left(\frac{\gamma_{20}}{2}C_2(0) + \Omega C_1(0)e^{-i\phi_L}\right)t\right], \qquad (20)$$

$$C_1(t) = e^{-\frac{\gamma_{20}}{2}t}\left[C_1(0) + \left(\Omega C_2(0)e^{i\phi_L} + \frac{2\Omega^2}{\gamma_{20}}C_1(0)\right)t\right]. \qquad (21)$$

Integrating Eq. (7) with the substitution of Eq. (20), by using (11) and employing the integration, after some algebra, yields

$$\rho_{00}(t) = (1 - e^{-\gamma_{20}t}) - \frac{\gamma_{20}^2 t^2 (1 + \cos\phi)}{2} e^{-\gamma_{20}t}, \qquad (22)$$

where ϕ is the phase difference, $\phi = \phi_p - \phi_L$ between the driving laser, ϕ_L, and the relative phase, ϕ_p between the states $|2\rangle$ and $|1\rangle$.

Entropy, $S(t)$ and magnitude $|C_1^*(t)C_2(t)|^2$ of the coherence, are depicted against $\gamma_{20}t$ for degree of excitation, $\theta = \pi/4$, double angles of the relative phase ϕ and different driving laser strengths Ω/γ_{20} in Fig.(1).

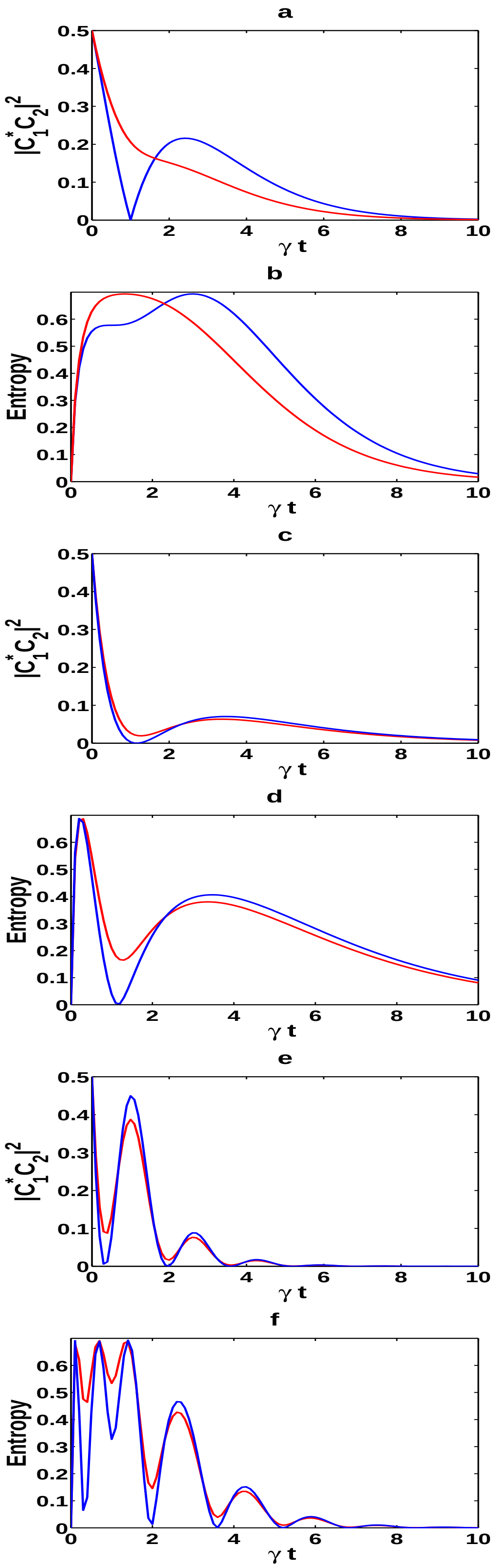

Fig. 1: Coherence $|C_1^* C_2|^2$, and Entropy, for $\phi = \pi/2$ (red), $\phi = 0$ (blue) and different values of $2\Omega/\gamma_{20} = 1, 0.8, 4.0$, where $\theta = \pi/4$.

From the figures, we see clearly the effect of the damping term $e^{-\gamma_{20}t}$, where decay to normal vacuum occurs after few oscillations, but with different degrees according to the change of the parameters ϕ and Ω/γ_{20}. It is noticed a rapid (when $\phi=\pi/2$) and slow (when $\phi=0$) decrease in the entropy S before decay to zero (field in the vacuum, the atom in the state $|0\rangle$) due to the different de-phasing of the off-diagonal coherences caused by environmental influences [42], Fig.(1a). When $\phi=0$, S maximum shifted left noticeably with amplitude remain fixed, see Figs. (1b). Note, the slow and rapid decrease in S is due to the time difference of populations of the symmetric and antisymmetric atomic states $\zeta|2\rangle\pm\eta|1\rangle$ to the upper state $|2\rangle$ which, accordingly, decays to ground state $|0\rangle$, thus, an early or late occurrence of energy exchange between the atom and reservoir, and so, slow or rapid full entanglement can occur. The effect when $2\Omega/\gamma_{20}<1$ is more pronounced. There is a point at which S doesn't decay completely and regenerates before decays to zero when $\phi=\pi/2$, Fig. (1d). At this point, coherence amplitude still have a value, because the symmetric state, $\zeta|2\rangle+\eta|1\rangle$, doesn't populate completely to the upper state $|2\rangle$. This is due to the weakness of the driving laser generates an intermediate level (level shift) rather than the upper state $|2\rangle$ at which full entanglement can occur. In other words, weak driving causes the symmetric atomic state $\zeta|2\rangle+\eta|1\rangle$ to decay to the ground state $|0\rangle$ before full population to the upper state $|2\rangle$, as a result, S increases and decays on a faster timescale and then regenerates before damping to zero, see Fig. (1d). Moreover, entanglement revives for longer timescal before decaying to zero in the case of weak driving laser. On $2\Omega/\gamma_{20}$ becomes more than unity, generally, the previous behavior is noticed except for, increasing driving laser strength induces oscillations in the coherence amplitude which makes S to decay and regenerate frequent times before damping to zero, see Figs. (1e,f).

5 Entanglement in the non-Markovian regime

5.1 Case (1): Entanglement dynamics through a PBS with an anisotropic dispersion relation

The decoherence of quantum system is always unavoidable because of the interactions with its local reservoir. To set up a reduced environmental effects, we now turn our attention to an action where the three-level atom is located within a PBS. In a real 3D dielectric crystal with an allowed point-group symmetry, the band edge wavevector varies as $\mathbf{k}$ is rotated throughout the Brillouin zone. Thus, a more realistic picture of the band edge behavior requires the incorporation of the Brillouin-zone anisotropy. In this case, the dispersion relation for the photons in the radiation reservoir is modified, with a gap(s) in the photon density of states. In the anisotropic effective mass approximation [43] the photon dispersion relation in a PBG material is given by

$$\omega_k \approx \omega_c + A(\mathbf{k}-\mathbf{k}_0)^2, \tag{23}$$

where, ω_c is the upper band edge frequency, $\mathbf{k}$ is the wavevector, and $A\approx f\omega_c/k_0$, with the dimensionless scaling factor f, measures the curvature of the dispersion curve [25]. For $(t-t')$ large enough to satisfy $\omega_c(t-t')\gg 1$, the memory kernel Eq. (9), reads [21]

$$F(t-t^{'}) = -\beta\,\frac{e^{i[\delta_c(t-t^{'})+\pi/4]}}{\sqrt{4\pi(t-t^{'})^3}}, \tag{24}$$

where $\beta^2=\omega_c\rho_{20}^2/(16f^3\omega_{20}^2)$, and the relative detuning of the upper and lower transitions from the band-edge is $\delta_c=\omega_c-\omega_{20}$.
Under this form of the memory kernel Eq. (24), applying the Laplace transforms and their inverse on Eqs.(5) and (8), the amplitudes $C_{1,2}(t)$ can be evaluated in the form

$$e^{-i\mu_L t}C_1(t) = e^{i\delta_c t}\sum_{m=1,2} a_{1,m}\, e^{i\varpi_m^2 t} + \frac{\beta\Omega e^{i\pi/4}\, e^{i(\delta_c+\mu_L)t}}{\pi}\int_0^\infty dx\, e^{-xt}\,\frac{F_1(x)}{I(x)}, \tag{25}$$

$$C_2(t) = e^{i\delta_c t}\sum_{m=1,2} a_{2,m}\, e^{i\varpi_m^2 t} + \frac{\beta e^{i\pi/4}\, e^{i(\delta_c+\mu_L)t}}{\pi}\int_0^\infty dx\, e^{-xt}\,\frac{F_2(x)}{I(x)}, \tag{26}$$

where

$$\varpi_{1,3} = -\sigma_1 \pm \sqrt{C_- - \sigma_1^2}, \quad \varpi_2 = \varpi_4^* = -\sigma_2 - i\sqrt{C_+ - \sigma_2^2}, \tag{27}$$

with

$$C_\pm = \pm r + \sqrt{r^2 + (\Omega^2 - \delta_c\mu_L - \delta_c^2)},$$

$$\sigma_{1,2} = \frac{1}{4}\left(\beta \pm \sqrt{\beta^2 - 4(\mu_L + 2\delta_c) + 8r}\right), \tag{28}$$

$$r = \tfrac{1}{6}\left(3(B-q)^{1/3} - 3(B+q)^{1/3} + \eta_1^2\right), \quad B = \sqrt{p^3+q^2}, \tag{29}$$

$$p = -\eta_1^2 + 3\eta_2, \qquad q = -3\left[\frac{\eta_1^3}{9} + \frac{1}{2}(\eta_1\eta_2 + 3\eta_3)\right], \tag{30}$$

$$\eta_1 = (\mu_L + 2\delta_c), \quad \eta_2 = \frac{\beta^2}{2}(\mu_L + 2\delta_c) + 4(\Omega^2 - \delta_c\mu_L - \delta_c^2), \tag{31}$$

$$\eta_3 = [\beta^2 - 4(\mu_L + 2\delta_c)](\Omega^2 - \delta_c\mu_L - \delta_c^2) - \frac{\beta^2}{4}(\mu_L + 2\delta_c)^2. \quad (32)$$

and

$$F_1(x) = \{[-x + i(\delta_c + \mu_L)]e^{i\phi_L}A_2(0) - \Omega C_1(0)\}\sqrt{x}, \quad (33)$$

$$F_2(x) = \{[-x + i(\delta_c + \mu_L)]e^{i\phi_L}A_2(0) - \Omega C_1(0)\}$$

$$(-x + i\delta_c + i\mu_L)\sqrt{x}, \quad (34)$$

$$I(x) = \{[-x + i(\delta_c + \mu_L)]^2 + \Omega^2\}^2 + i\beta^2[-x + i(\delta_c + \mu_L)]^2. \quad (35)$$

The coefficients $a_{(1,2),m}$ where $m = 1,2$, corresponding to w_m, which depends on Ω, δ_c and $C_j(0)$, are given by the expressions

$$a_{1,m} = \frac{2\varpi_m}{\varpi_{mkln}}[(\varpi_m^2 + \beta\varpi_m + \delta_c)C_1(0) - i\Omega e^{i\phi_L}A_2(0)], \quad (36)$$

$$a_{2,m} = \frac{2\varpi_m}{\varpi_{mkln}}[(\varpi_m^2 + \delta_c + \mu_L)A_2(0) + i\Omega e^{-i\phi_L}C_1(0)], \quad (37)$$

where, $k,l,n = 1,2,3,4, m = 1,2$, and $m \neq k \neq l \neq n$, and

$$\varpi_{mkln} = \varpi_{mk}\varpi_{ml}\varpi_{mn}; \quad \varpi_{xy} = (\varpi_x - \varpi_y), \quad (38)$$

Since ϖ_1 is real, and ϖ_2 is complex (with negative real and imaginary parts), the first terms in the right-hand side of equations (**??**) and (26) are non-decaying oscillatory terms, whereas the second term is also oscillatory but decays exponentially to zero as $t \to \infty$. The last terms containing the integral decay to zero as $t \to \infty$ faster than the second term, so their contribution to the interaction is eventually trivial and can be ignored, in this case the amplitudes $C_1(t)$ and $C_2(t)$ read

$$C_1(t) \approx e^{i(\delta_c+\mu_L)t} \sum_{m=1,2} a_{1,m}\, e^{i\varpi_m^2 t}, \quad (39)$$

$$C_2(t) \approx e^{i\delta_c t} \sum_{m=1,2} a_{2,m}\, e^{i\varpi_m^2 t}. \quad (40)$$

Figure (2), illustrates the dynamical evolution of $|2\rangle$ population $|C_2|^2$ and entropy S, where the effects of memory kernel function on the entanglement are considered, for same initial relative phase ϕ as in last figures, but the driving laser strength is now $\Omega/\beta^2 = 2$, where, we preserved the atom in an equal superpostion; $\theta = \pi/4$, and the detuning of the transition frequency from the band-edge is assumed to have values $\delta_c/\beta^2 = 0,1$ while various detunings from driving laser, μ_L/β^2, are considered.

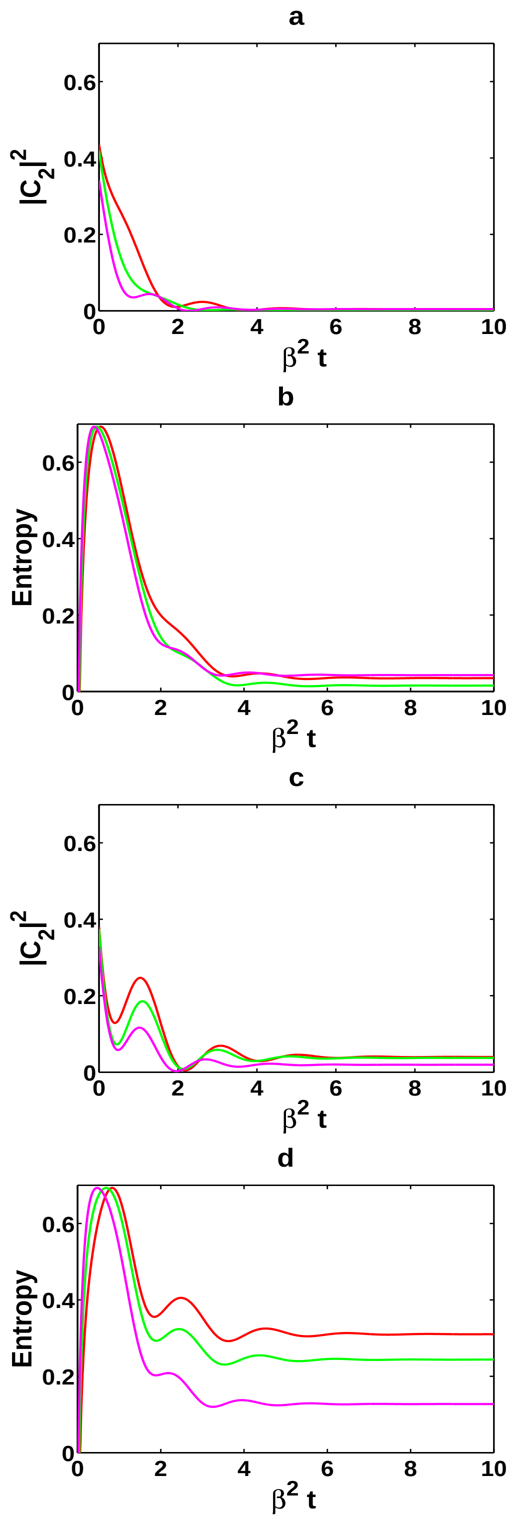

Fig. 2: Population $|C_2|^2$, and Entropy, when $\Omega/\beta^2 = 2.0$ and $\theta = \pi/4$, and $\mu_L/\beta^2 = 0.0$ (red), $\mu_L/\beta^2 = 1.0$ (green), $\mu_L/\beta^2 = 2.0$ (violet), for $\delta_c/\beta^2 = 1.0$ and different values of $\phi = \pi/2, \pi/4, 0$ and $-\pi/2$. For (i, j), $\delta_c/\beta^2 = 0$ and $\phi = -\pi/2$.

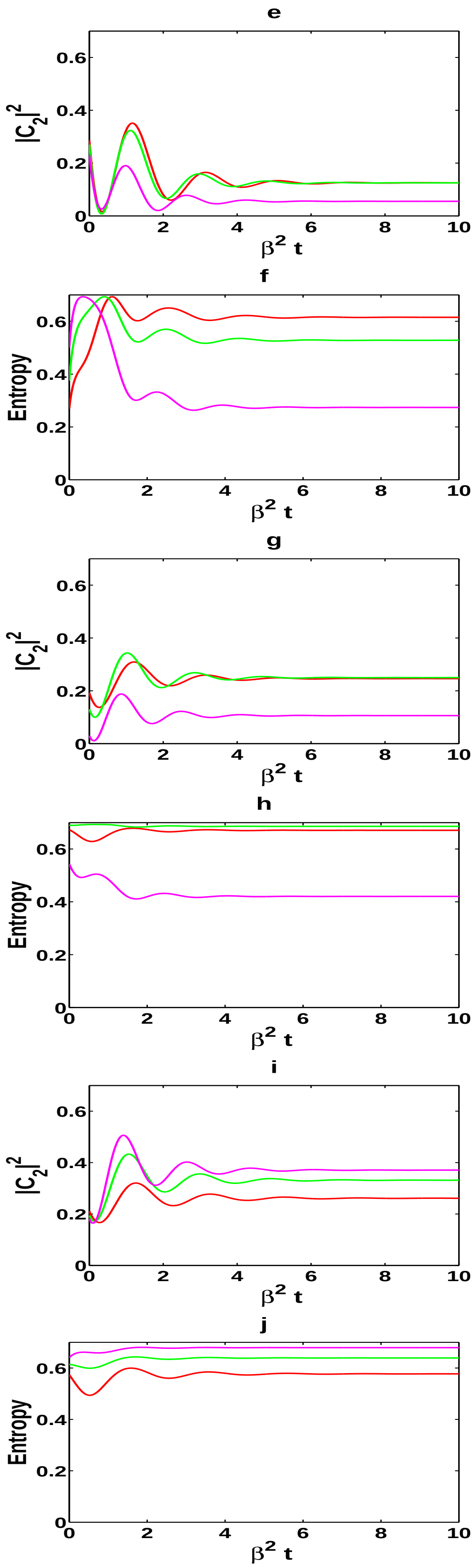

Fig. 3: Fig. 2 continued.

We note that, for $\phi = \pi/2$, a highly non-Markovian decay of both $|C_2|^2$ and S is exhibited where the difference for varying μ_L/β^2 is negligible, Fig. (2a,b), while for other ϕ values, there is no decay to zero of either $|C_2|^2$ or S. This can be illustrated as follows: As it is known from the coupling of a two-level atom to the PBS reservoir, the dressing of the atom by its own radiation causes splitting of the atomic levels. This splitting is sufficiently strong to push one level of the doublets outside the gap and the other inside. The dressed state outside the gap looses all its population in the long-time limit, while the one inside the gap is protected from dissipation and thus is stable [44]. This can be clear from Eq. (40) which shows that level $|2\rangle$ is split into two dressed states. This dressed-state splitting is the combined effect of vacuum-field Rabi splitting by the gap [45] and the Autler-Townes splitting [46] by the external field. The dressed states occur at frequencies [noting that root ϖ_1 is real, whereas $\mathrm{Re}(\varpi_2^2) < 0$]

$$\omega_{20} - [\delta_c + \mathrm{Im}(i\varpi_1^2)] = \omega_c - \mathrm{Im}(i\varpi_1^2) = \omega_c - \varpi_1^2 \quad (41)$$

$$\omega_{20} - [\delta_c + \mathrm{Im}(i\varpi_2^2)] = \omega_c - \mathrm{Im}(i\varpi_2^2)$$

$$= \omega_c - \mathrm{Re}(\varpi_2^2) = \omega_c + |\mathrm{Re}(\varpi_2^2)| \quad (42)$$

The dressed state at the frequency $\omega_c + |\mathrm{Re}(\varpi_2^2)|$ lies outside the gap and decays at a rate of $\mathrm{Im}(\varpi_2^2)$ which resulted in the highly non-Markovian decay of the atomic population, and as a result, a rapid decay of entanglement. In contrary, the dressed state at frequency $\omega_c - \varpi_1^2$ lies inside the gap and corresponds to the photon-atom bound dressed state with no decay in time, which means very different spontaneous emission dynamics -from free space- that depends strongly on the detuning $\delta_c = \omega_{20} - \omega_c$ of level $|2\rangle$ from the upper band edge. In other words, as the relative phase ϕ decreases, thus, the atom becomes more near to be in a superposition of its two states. This is a novel behavior, due to the fact that both transitions and not only one, are coupled to the same structured continuum and we have the formation of a ”photon+atom” bound state [26,43,25,44,32], which exhibits population trapping in both excited states, in the long-time limit [44]. In this case, specially for symmetric and antisymmetric states $\zeta|2\rangle \pm \eta|1\rangle$, S grows up clearly and reaches its steady-state value more quickly for $\mu_L/\beta^2 \in [0,1]$. This is due to the possibility of stimulated transitions between either symmetric or antisymmetric states and state $|2\rangle$. Note, an optimal entanglement with the highest steady-state maximum can be reached on negative relative phase ϕ while $\mu_L/\beta^2 = \delta_c/\beta^2 = 1$, see Figs. (2e,f) and (2g,h) , while for tuned ω_{20} into the gap, this feature can be seen when $\mu_L/\beta^2 > 1$, which means that, pumping with classical laser of matching frequency may suppresses efficiently the effect of the detuning from the band gap δ_c/β^2, Fig. (2i,j). In the language of dressed states, the oscillations in $|C_2|^2$, hence in S, reflect the interference between the dressed states of the atom. The new feature that the PBS brings is in the creation of long-lived correlations between the modified reservoir and the atom that depend crucially on both PBS and driving laser parameters and can increase above its initial value. We see from the figures, how the correlation evolves to this steady-state. This is due to the phenomenon of population trapping which, in consequence, is due to the presence of a PBG material and is absent in free space. This trapped population gives rise to the asymptotic correlation between the atom and the field [9,19].

5.2 Case (2): Non-Markovian Entanglement in the stationary regime

In the long-time limit, only the first terms in equations (39) and (40) remain dominant, since ϖ_1 is real whereas ϖ_2 is complex with a negative real part. The steady-state amplitudes $C_j(t)$ of the upper levels $|2\rangle$ and $|1\rangle$ are thus given by

$$C_1^{st} = a_{1,1} = \frac{2\varpi_1}{\varpi_{1kln}}[(\varpi_1^2 + \beta\varpi_1 + \delta_c)C_1(0) - i\Omega e^{i\phi_L}C_2(0)] \tag{43}$$

$$C_2^{st} = a_{2,1} = \frac{2\varpi_1}{\varpi_{1kln}}[(\varpi_1^2 + \delta_c + \mu_L)C_2(0) + i\Omega e^{-i\phi_L}C_1(0)] \tag{44}$$

Putting in mind that the quantity $2\varpi_1/\varpi_{1kln}$ in Eqs. (43) and (44) is real, as ϖ_1 is real and ϖ_{1kln} is real too, leads us to expect that the development of both steady-state population, $|C_2^{st}|^2$, and steady-state entropy, S^{st}, will evolve maximally or minimally according the change in ϕ sign, while the shape of their behavior will be determined and controlled by the driving laser strength Ω. The detailed analysis is given in Figs. (4 and 5).

Figures (4) and (5) show, respectively, the variation of the stationary state evolution with respect to the detuning δ_c/β^2 and driving laser strength parameter Ω/β^2, where atomic degree of excitation $\theta = \pi/4$ remains fixed for all plots.

Generally, we can notice that, for $\phi = \pi/2$, the detuning μ_L/β^2 controls $|C_2^{st}|^2$ and S^{st} to behave similar to each other, see Figs. (4a,b, 4g,h, 5a,b and 5g,h), where as $|C_2^{st}|^2$ exhibits increasing, S^{st} shows increasing too, and vice versa for $\phi = 0$, Figs. (4c,d, 4i,j, 5c,d and 5i,j).

Figures (4e,f, 4k,l, 5e,f and 5k,l), where $\phi = -\pi/2$, show increase in both $|C_2^{st}|^2$ and S^{st} when μ_L/β^2 increases. A fine look at these figures can shed light on some important details and give us a deeper insight into the efficient effects of these parameters.

First of all, for a strong driving laser, $\Omega = 3\beta^2$, as δ_c/β^2 increases from zero (that is, as level $|2\rangle$ is pushed farther away from the band edge into the continuum), $|C_2^{st}|^2$ initially increases and attains its maximum value at about $\delta_c \approx 0.5\beta^2$ before it begins to decrease very rapidly, while S^{st} appears to be less sensitive in this stage, specially for $\delta_c/\beta^2 < 0$, where it decays very slowly from its stationary value (of about 0.69 at $\delta_c = -2\beta^2$). At the point where $|C_2^{st}|^2$ begins to decrease, S^{st} decays very rapidly too, Fig. (4c,d). This is because, there is a fractionalized $|C_2^{st}|^2$ on the excited state $|2\rangle$ even when the bare excitation frequency of this level lies outside of the PBG, but not far from the band edge [21,30].

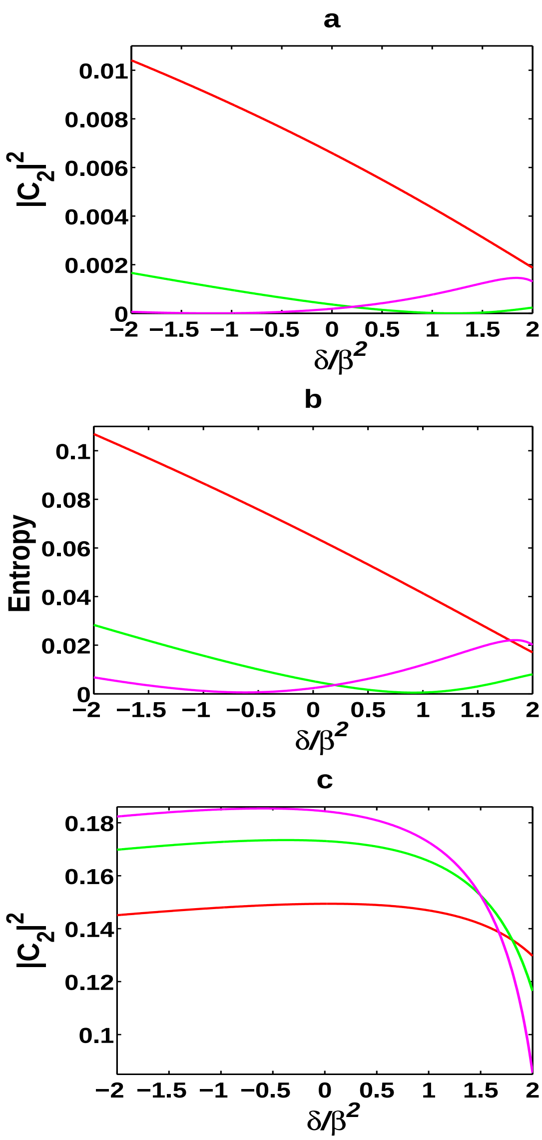

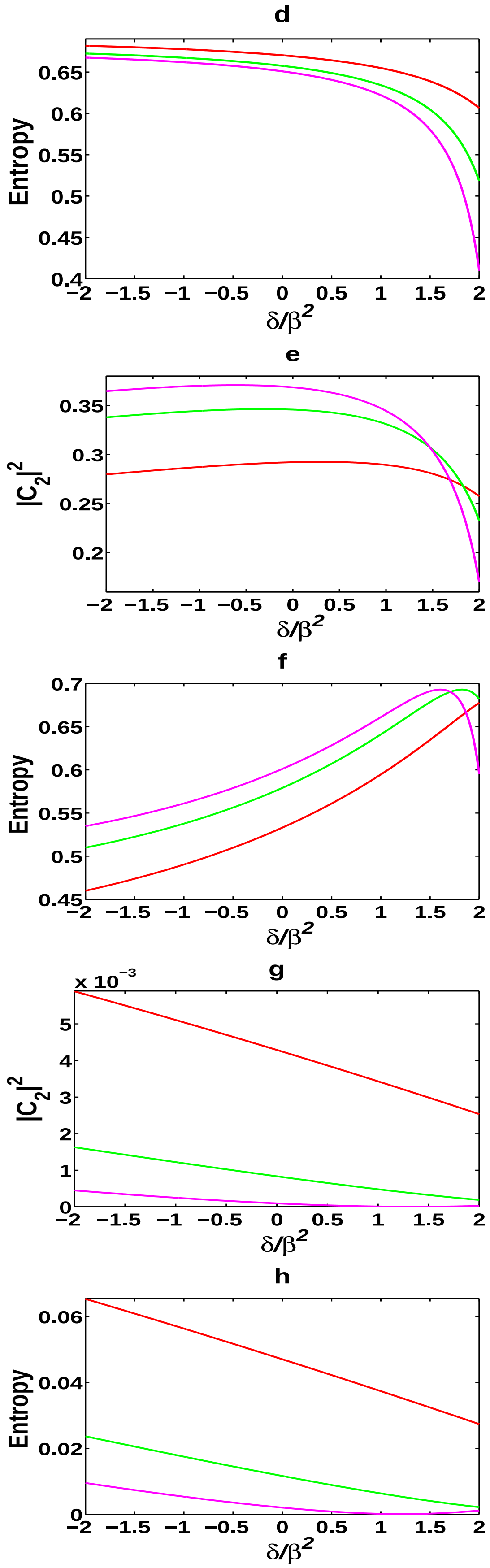

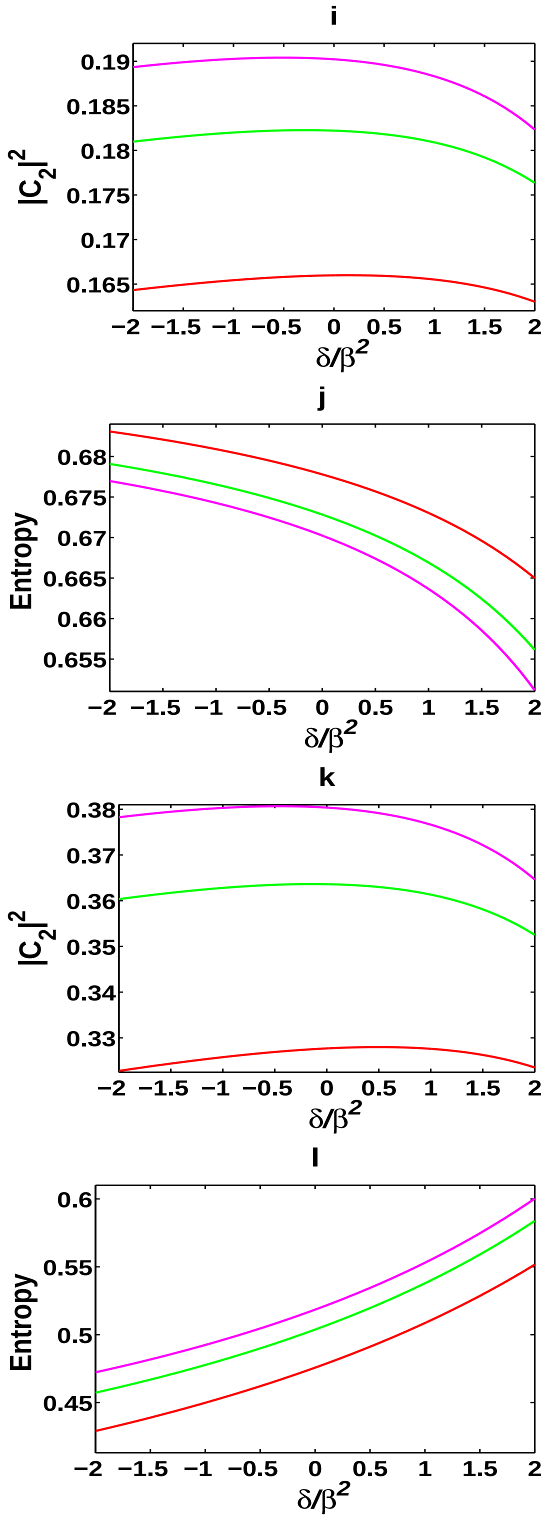

Fig. 4: Population $|C_2|^2$, and Entropy in the steady state against δ_c/β^2, when $\theta = \pi/4$ and $\mu_L/\beta^2 = 0.0$ (red), $\mu_L/\beta^2 = 1.0$ (green), $\mu_L/\beta^2 = 1.5$ (violet), for different values of $\phi = \pi/2, 0, -\pi/2$, where $\Omega/\beta^2 = 3.0$ for (a-f) and $\Omega/\beta^2 = 5.0$ for (g-l).

In other words, as ω_{20} is detuned further into the gap (i.e. as δ_c/β^2 becomes more negative), a greater fraction of the light is localized in the gap dressed state. Conversely, as ω_{20} is moved out of the gap, total emission intensity from the decaying dressed state is increased [25, 47].

A comparison with Fig. (5i,j), where both $|C_2^{st}|^2$ and S^{st} are function of Ω/β^2, it is apparent that it is a limiting case of Fig. (4c,d), where both $|C_2^{st}|^2$ and S^{st} begin to increase to attain stationary state in the limit of stronger driving laser. This is a general and common property that can be noticed easily by comparing Figs. [(4a,b) and (5g,h)], [(4e,f) and (5k,l)], [(4i,j) and (5c,d)] and [(4k,l) and (5e,f)]. This is not the whole thing, where the effect when the driving laser is detuned farther from ω_{21} is, however, interesting. For fixed driving strength, the point at which S^{st} begins to decrease from its maximum value, of about 0.69 at about $\delta/\beta^2 = 1.5$, as μ_L/β^2 increases, is shifted left noticeably, see Figs. (4e,f), while an opposite situation can be noticed for fixed detuning from the upper band edge δ/β^2, where, this point, at about $\Omega = 3.5\beta^2$, is shifted right remarkably, see Figs. (5k,l).

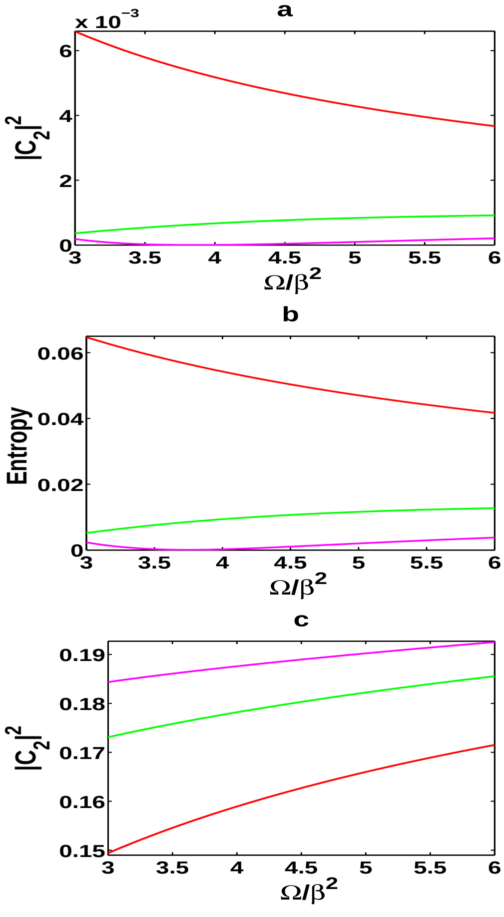

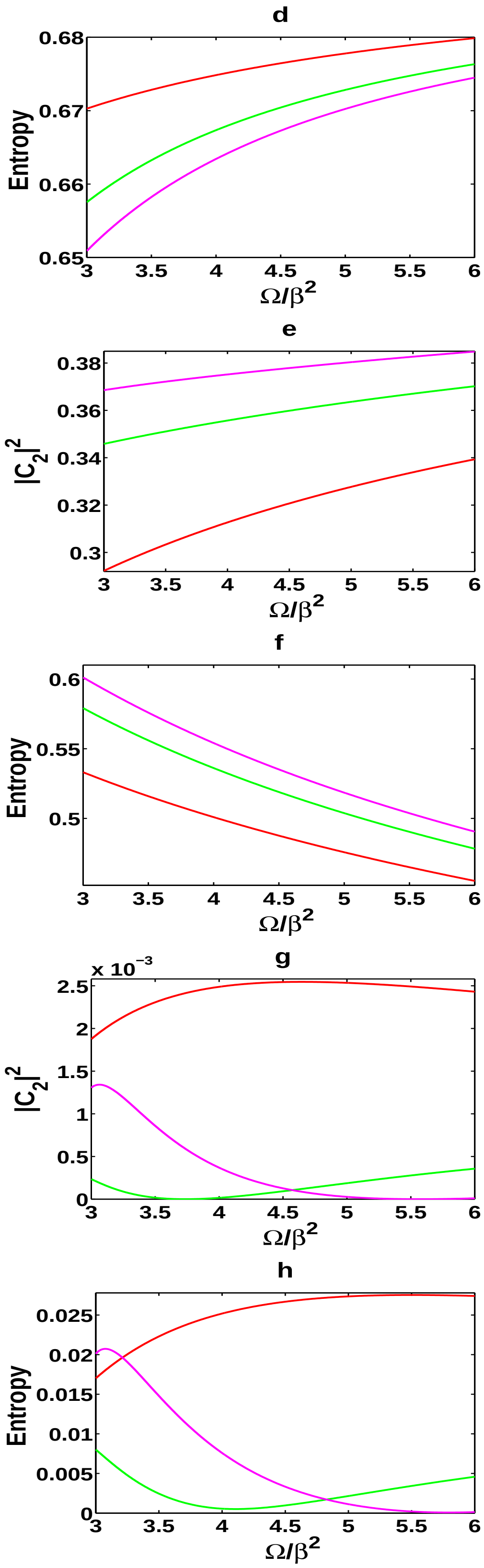

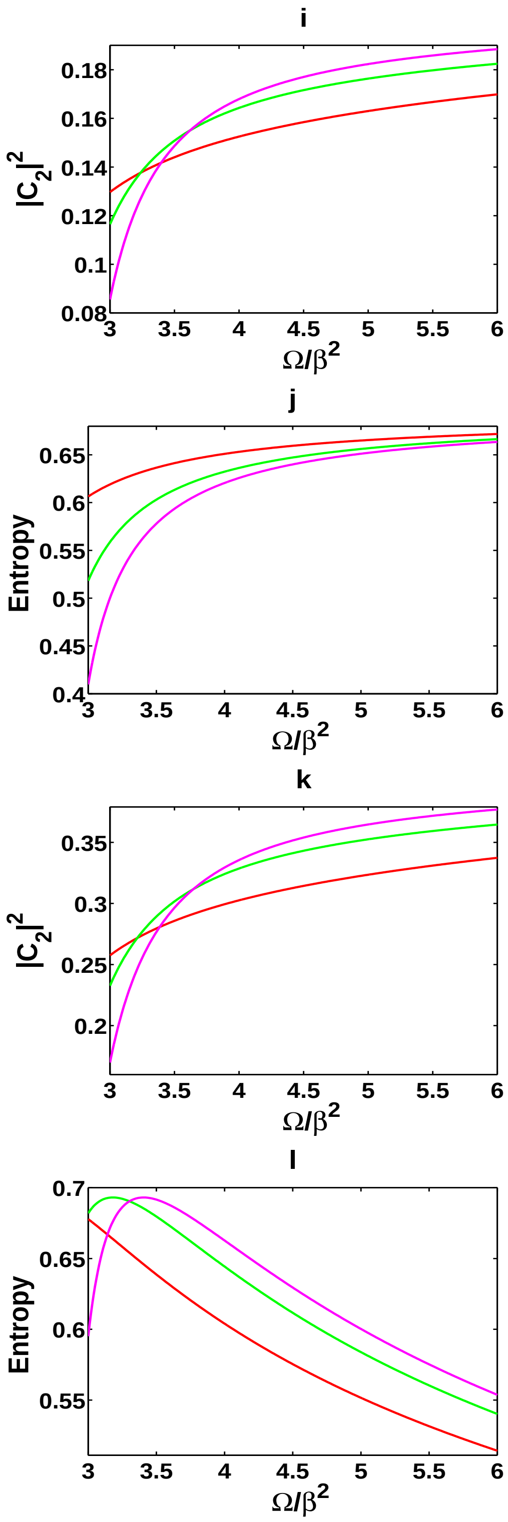

Fig. 5: Population $|C_2|^2$, and Entropy in the steady state against Ω/β^2, where $\theta = \pi/4$ and $\mu_L/\beta^2 = 0.0$ (red), $\mu_L/\beta^2 = 1.0$ (green), $\mu_L/\beta^2 = 1.5$ (violet), for different values of $\phi = \pi/2, 0, -\pi/2$, where $\delta_c/\beta^2 = 0.0$ for (a-f) and $\delta_c/\beta^2 = 2.0$ for (g-l).

6 Conclusion

In summary, we present a scheme for preserving entanglement in the steady state between parts of a bipartite system of Λ-type three-level atom coupled to a vacuum reservoir. To achieve this goal, the upper levels of the atom were coupled through a classical control laser while the reservoir was engineered through locating the atom into PBS, that allows for the formation of non-Markovian effects. The analysis showed that, engineering the reservoir, initial laser pulse strength, and detuning from upper band edge frequency of the PBS, play a crucial role in this process. We demonstrated that, opposite to interaction in free space (the non-Markovian effect is neglected), where entanglement sudden death (ESD) is dominant, the existence of bound state of atom and its reservoir and the non-Markovian effects supresses decoherence noticeably, where, entanglement preservation can be simply achieved. Moreover, the process interplay near an off-resonance interaction with upper band edge frequency is more advantageous than that operating near on-resonance interaction. In the longtime limit, the stationary entanglement evolves towards maxima or minima according to the change in the sign of the relative phase regardless of the value of the relative detuninig between the upper levels and the pump laser pulse, while its shape will be controlled by the driving laser strength.

References

[1] Schrödinger E, *Naturwissenschaften*, **23**, 807, 823, 844 (1935).
[2] Einstein A, Podolsky B, and Rosen N, *Phys. Rev.*, **47**, 777 (1935).
[3] Horodecki R, Horodecki P, Horodecki M and Horodecki K, *Rev. Mod. Phys.*, **81**, 865 (2009).
[4] M. Abdel-Aty and M. J. Everitt, Eur. Phys. J. B., **74**, 81 (2010) .
[5] A.-S. F. Obada, M. R. B. Wahiddin and M. Abdel-Aty, Optics Commun., **281**, 6019 (2008).
[6] M. Abdel-Aty, Optics Commun., **275** , 129 (2007).
[7] Nielsen M A and Chuang I L, *Quantum Computation and Quantum Information*, (Cambridge University Press, Cambridge, UK,) (2000).
[8] Breuer H P and Petruccione F, *The Theory of Open Quantum Systems*, (Oxford University Press, Oxford,) (2002).
[9] Ekert A K and Phoenix S J D, *J. Mod. Opt.*, **38**, 19 (1991).
[10] Hartmann L, Dür W and Briegel H-J, *New J. Phys.*, **9**, 230 (2007).
[11] López C E, Romero G and Retamal J C, *arXiv:1007.1951v1*, [quant-ph], (2010).
[12] Suzuki J, Miniatura C, and Nemoto1 K, *arXiv:1002.4716v2*, [quant-ph], (2010).
[13] Agudelo E, Rodriguez B A, Fonseca-Romero K M, *arXiv:1002.4242v1*, [quant-ph], (2010).

[14] Sun Z, Wang X G and Sun C P, *Phys. Rev.*, **A75**, 062312 (2007) ; Yu T and Eberly J H, *Opt. Commun.*, **fg.203**, 676 (2010) ; Cao X F and Zheng H, *Phys. Rev.*, **A77**, 022320 (2008).
[15] Xu Z Y and Feng M, *Phys. Lett. A*, **373**, 1906 (2009) ; Wang X G, Miranowicz A, Lin Y X, Sun C P and Nori F, *Phys. Rev.*, **A81**, 022106 (2010) ; Siomau M and Fritzsche S, *Phys. Rev.*, **A82**, 062327 (2010).
[16] Szallas A and Troiani F, *Phys. Rev.*, **B82**, 224409 (2010) .
[17] Maziero J, Werlang T, Fanchini F F, Celeri L C, and Serra R M, *Phys. Rev.*, **A81**, 022116 (2010); Erbe B and Schliemann J, *Phys. Rev.*, **B81**, 235324 (2010) ; Wang H T, Li C F, Zoou Y, Ge R C, and Guo G C, *Physica A*, **390**, 3183 (2011) .
[18] Li J G, Zou J and Shao B, *Phys. Lett.* A, **375**, 2300 (2011) ; Liao C G, Yang Z B, Chen Z H, and Luo C L, *Commun. Theor. Phys.*, **54**, 667 (2010); Fu C J, Zhu Q S and Wu S Y, *Commun. Theor. Phys.*, **53**, 1072 (2010) ; Shi Z G, Chen X W, Wen W, Xiang S H and Song K H, *Commun. Theor. Phys.*, **56**, 317 (2011), .
[19] Tong Q-J, An J-H, Luo H-G and Oh C H, *Phys. Rev.* A, **81**, 052330 (2010).
[20] Tong Q-J, An J-H, Luo H-G and Oh C H *Quantu. Inf. Comput.*, **11**, 0874 (2011).
[21] Woldeyohannes M and John S, *J. Opt. B: Quantum Semiclass. Opt.*, **5**, R43 (2003).
[22] Haake F, *Statistical Treatment of Open Systems by Generalized Master Equations*, (Springer Tracts of Modern Physics,) (Berlin: Springer) **66**, (1973).
[23] Meystre P and Sargent M, *Elements of Quantum Optics*, (New York: Springer); Scully M O and Zubairy S, (1997), *Quantum Optics*, (Cambridge: Cambridge University Press), (1991).
[24] Zhou J , Wu C, Zhu M and Guo H, *arXiv:0904.1658v3*, [quant-ph], (2009).
[25] John S and Quang T, *Phys. Rev.*, **A50**, 1764 (1994).
[26] Kofman A G, Kurizki G and Sherman B, *J. Mod. Opt.*, **41**, 353 (1994).
[27] Zhang J and Xu J, *Opt. Commun.*, **282**, 3652 (2009); Zhang Y, Man Z and Xia Y, *J. Phys. B*, **42**, 095503 (2009); Friedler I, Kurizki G and Petrosyan D, *Europhys. Lett.*, **68**, 625 (2004).
[28] Rossatto D Z, Werlang T and Villas-Boas C J, *arXiv:1102.0073v1*, [quant-ph], (2011).
[29] John S, *Phys. Rev. Lett.*, **53**, 2169 (1984); John S, *Phys. Rev. Lett.*, **58**, 2486 (1987).
[30] Yablonovitch E, *Phys. Rev. Lett.*, **58**, 2059 (1987); Bykov V P, *Sov. J. Quantum Electron.* **4**, 861 (1975).
[31] Zhu S Y, Chen H and Huang H, *Phys. Rev. Lett.*, **79**, 205 (1997); Quang T, Woldeyohannes M, John S, Agarwal G S, *Phys. Rev. Let.*, **79**, 5238 (1997); Bay S, Lambropoulos P, *Opt. Com.*, **146**, 130 (1998).
[32] Paspalakis E, Kylstra N J and Knight P L, *Phys. Rev.*, **A60**, R33 (1999).
[33] Wootters W K, *Phys. Rev. Lett.*, **80**, 2245 (1998).
[34] Xiang H, Jin-Qiao S, Jian S and Shi-Qun Z *Commun. Theor. Phys.*, **57**, 29 (2012).
[35] Vidal G and Werne R F, *Phys. Rev.*, **A65**, 032314 (2002).
[36] Bennett C H, DiVincenzo D P, Smolin J A, and Wootters W K, *Phys. Rev.*, **A54**, 3824 (1996); Vedral V and Plenio M B, *Phys. Rev.*, **A57**, 1619 (1998).
[37] von Neumann J, *Götingger Nachr.*, 273 (1927).
[38] Phoenix S J D, Knight P L, *Ann. Phys.*, (N. Y.), **186**, 381 (1988); Phoenix S J D, Knight P L, *Phys. Rev.*, **A44**, 6023 (1991); *Phys. Rev. Lett.*, **66**, 2033 (1991).
[39] Ateto M S, *Int. J. Theo. Phys.*, **49**, 276 (2010).
[40] Popescu S, *Phys. Rev. Lett.*, **72**, 797 (1994).
[41] Vedral V, Plenio M B, Rippin M A and Knight P L, *Phys. Rev. Lett.*, **78**, 2275 (1997).
[42] Zurek W H, *Phys. Rev.* D, **24**, 1516 (1981); Walls D F and Milburn G J, *Phys. Rev.*, **A31**, 2403 (1985); Phonix S J D, *Phys. Rev.*, **A41**, 5132 (1990).
[43] John S and Wang J, *Phys. Rev. Lett.*, **64**, 2418 (1990); John S and Wang J, *Phys. Rev. Lett.*, **43**, 12772 (1991).
[44] Nikolopoulos G M and Lambropoulos P, *arXiv:0002051v1*, [quant-ph], (2000).
[45] Raizen M G, Thomson R J, Brecha R J, Kimbel H J and Carmichael H J, *Phys. Rev. Lett.*, **63**, 240 (1989).
[46] Autler H and Townes C H, *Phys. Rev.*, **100**, 703 (1955).
[47] Vats N and John S, *Phys. Rev.*, **A58**, 4168 (1998).